

DOI: 10.1002/adma.200700917

Long-Range Resonant Energy Transfer for Enhanced Exciton Harvesting for Organic Solar Cells**

By Shawn R. Scully, Paul B. Armstrong, Carine Edder, Jean M. J. Fréchet, and Michael D. McGehee*

Exciton harvesting is of fundamental importance for the efficient operation of organic photovoltaic devices. The quantum efficiencies of many organic and hybrid organic-inorganic devices are still limited by low exciton harvesting efficiencies. This problem is most apparent in planar heterostructures that suffer from a direct tradeoff between light absorption and exciton harvesting. The bulk heterojunction concept^[1,2] was designed to alleviate the problem of limited exciton migration by intimately blending the donor and acceptor phases on the nanometer length scale. In some polymer/fullerene systems, such as poly(2-methoxy,5-(3,7-dimethyloctyloxy)-1,4-phenylenevinylene) (MDMO-PPV)/(6,6)-phenyl C61-butyric acid methyl ester (PCBM), time resolved spectroscopy shows the photoinduced formation of the radical anions and cations on femtosecond timescales.^[3] This ultrafast formation of the polaron signature is only possible if every exciton is formed on a polymer chain segment that is immediately adjacent to one or more fullerene molecules. However, in other systems, very large domains prevail and, consequently, exciton harvesting is inefficient.^[4] This has made the fabrication of efficient devices incorporating new materials difficult because each new material leads to a new morphology with its own characteristic length scale. The ordered bulk heterojunction architecture is intended to alleviate these issues by using a pre-patterned nanostructured scaffold^[5–7] that has been engineered to have both straight pathways to the electrodes to ensure efficient carrier collection, and controlled domain size to ensure efficient exciton harvesting. Recently, chain alignment has been shown to be promoted for regioregular poly(3-hexyl thiophene) (RR-P3HT) in straight nanopores of anodic alumina leading to a 20-fold increase in hole-mobility in these struc-

tures.^[8] For solar cell applications, higher mobilities reduce the effects of space charge^[9] and increase the probability of separating the geminate pair formed immediately after exciton dissociation.^[10–13] While the ordered bulk heterojunction architecture shows promise, existing structures have domains too large^[14,15] for efficient exciton harvesting with singlet diffusion lengths only ca. 3–8 nm.^[16–18] At this time, few alternatives other than nanostructuring have been proposed to increase exciton harvesting. Triplet excitons have been shown to have large diffusion lengths due to their long lifetimes,^[18–20] but except in a few examples^[21,22] this usually comes at the expense of a loss in energy of 0.4–0.8 eV associated with intersystem crossing between the photoexcited singlet to the first excited triplet.^[23–25] At present, the direct engineering of singlet materials that have large diffusion lengths remains elusive due to the inherent disorder of most organic thin film materials. In this communication, we present theory and experiments that support a scheme to harvest singlet excitons over 25 nm away from the donor-acceptor interface in organic solar cells using resonant energy transfer. These results represent dramatic improvements over previous findings^[26] and show that this scheme holds promise for the future design of highly efficient organic photovoltaics.

Resonant energy transfer has been used in organic photovoltaics to broaden the absorption spectrum^[30] and is thought to play a role in harvesting excitons in bulk heterojunction cells.^[31,32] However, the intentional use of hetero-energy transfer to achieve longer range exciton harvesting in photovoltaics had largely been overlooked until recently.^[26] Since the rate of transfer between two chromophores is proportional to $1/r^{6[28]}$ and the characteristic distance of transfer is typically only 2–4 nm, it is often assumed that, at best, excitons could be harvested across this marginally larger distance when energy transfer is used. However, both the relevant geometry and a proper accounting of rates are of the utmost importance in determining absolute transfer rates. In a heterostructure, the exciton in the donor phase can be transferred to any one of the chromophores in the acceptor film. Therefore, to obtain the total rate of transfer we must sum over all possible transfer events. This is shown schematically in Figure 1.

The rate of transfer from an excited chromophore to a 2D sheet varies as $1/x^{4[33]}$ and to a 3D seminfinitive array as $1/x^3$,^[16,33] where x has been chosen as a distance from a planar interface rather than a radial distance. Energy transfer for the geometrically relevant structures is many times more efficient than would be the case between two isolated chromophores. This relaxed distance dependence has been previously recog-

[*] Prof. M. D. McGehee, S. R. Scully
Department of Materials Science and Engineering, Stanford University
Stanford, CA 94305-2205 (USA)
E-mail: mmcgehee@stanford.edu

P. B. Armstrong, Prof. J. M. J. Fréchet
Department of Chemistry, University of California at Berkeley
Berkeley, CA 94720-1460 (USA)

Dr. C. Edder, Prof. J. M. J. Fréchet
The Molecular Foundry, Lawrence Berkeley National Laboratory
Berkeley, CA 94720-8298 (USA)

[**] Support of this work by the Materials Sciences and Engineering Division of the U.S. Department of Energy under Contract No. DE-AC02-05CH11231 and the Center on Polymer Interfaces and Macromolecular Assemblies (CPIMA) is gratefully acknowledged. We also thank the DOW Chemical Company for providing materials.

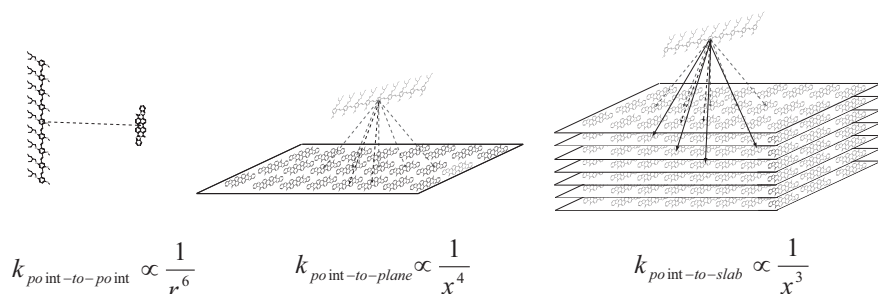


Figure 1. Schematics showing representations of three different geometries for energy transfer, point-to-point (left), point-to-plane (center), and point-to-slab (right). For simplicity, only the excited chromophore is drawn on the donor side, while in physically relevant systems the excited chromophore is embedded in a 3D matrix of non-excited donor chromophores. Small D-A separation distances were chosen to emphasize the various possible transfer pathways. At larger distances (> 10 nm) the donor would look like a point and the acceptor planes and slabs would appear to be continuous rather than discrete as above. The arrows show representative energy transfer pathways. Point-to-point corresponds to the situation where both donor and acceptor chromophores are randomly dispersed in a matrix. Point-to-plane corresponds to the case where a donor chromophore can couple to a monolayer of acceptor molecules. Point-to-slab corresponds to the case where a donor chromophore can couple to a 3D array of acceptor molecules.

nized for its importance in describing excitation transfer to metal films,^[33–35] between dyes in layered Langmuir–Blodgett structures,^[36–39] and in heterostructure OLEDs.^[40]

We recently reported device results using regioregular poly(3-hexylthiophene (RR-P3HT) as the energy donor and the low bandgap polymer poly(*N*-dodecyl-2,5,-bis(2'-thienyl)-pyrrole-2,1,3-benzothiadiazole) (PTPTB)^[41,42] as the energy acceptor.^[26] We showed a near threefold enhancement in the photocurrent compared to a titania/RR-P3HT bilayer device and exciton harvesting measurements showed that excitons could be harvested from nearly 10 nm away from the heterointerface. RR-P3HT is well-known to have a low luminescence quantum yield^[43] due to tight π - π stacking and efficient aggregate/excimer formation that limits the usefulness of resonant energy transfer in this system by reducing the Förster radius. We will now quantitatively explain exciton harvesting using hetero-energy transfer and show simulations and experiments that demonstrate dramatic improvements upon these early results.

Exciton migration is usually modeled assuming a random walk, perfect quenching at the donor-acceptor interface, and perfect reflecting at the non-quenching interface.^[16,18,29,44] For the 1D case, the continuity equation for the exciton density, n , and the idealized boundary conditions are given in Equations 1.1–1.3.

$$\frac{\partial n}{\partial t} = D \frac{\partial^2 n}{\partial x^2} - \frac{n}{\tau} + G(x) \quad (1.1)$$

$$n|_{\text{quench}} = 0 \quad (1.2)$$

$$-D \left. \frac{\partial n}{\partial x} \right|_{\text{nonquenching}} = 0 \quad (1.3)$$

The first term on the right in Equation 1.1 corresponds to exciton diffusion with diffusivity, D . The second term is the natural decay of the exciton with lifetime τ and the third is the exciton generation profile, $G(x)$. Equation 1.2 is the boundary condition for a perfectly quenching interface (which the D-A heterointerface ideally acts as) whereas Equation 1.3 is the condition for a perfectly reflecting interface. As alluded to earlier, because of disorder, singlet migration is not actually a true random walk.^[45–47] Consequently “exciton diffusion” is a misleading term. However, it turns out that steady-state exciton harvesting measurements can still be well-described using this model and an effective diffusion length, $L_D = \sqrt{D\tau}$, can be extracted that consistently models exciton harvesting in a variety of experiments. In this way L_D is more of an

empirical factor that describes average exciton migration properties. When a donor-acceptor interface is present at one of the planar boundaries of the organic film, three quarters of the excitons will be harvested from an organic film when the film thickness is equal to L_D and when the spatial generation of excitons is a constant.

Following this empirical spirit, we can simulate exciton harvesting when hetero-energy transfer is possible as an additional exciton migration pathway. Equation 2.1 is a modified continuity equation, which includes an extra term corresponding to exciton harvesting by long-range resonant energy transfer with the rate given by Equation 2.2.

$$\frac{\partial n}{\partial t} = D \frac{\partial^2 n}{\partial x^2} - \frac{n}{\tau} - k_F \cdot n + G(x) \quad (2.1)$$

$$k_F(x) = \frac{C_A}{\tau} \frac{\pi R_0^6}{6 x^3} \quad (2.2)$$

where R_0 is the Förster radius^[28] and C_A is the acceptor chromophore density.^[48] Equation 2.1 is numerically solved to calculate the fraction of excitons harvested as described previously^[16] using the same boundary conditions as 1.2 and 1.3.

Figure 2a shows exciton harvesting as a function of energy donor film thickness assuming a constant generation rate, and an exciton diffusion length of 5 nm. Curves are shown for the case where there is only exciton diffusion as well as for cases involving energy transfer in addition to intrinsic exciton diffusion. An important parameter, which determines the shape of these curves is the Förster radius, R_0 . The Förster radius is a measure of the strength of coupling between donor and acceptor chromophores. Stronger coupling results in a larger R_0 , and consequently a greater fraction of excitons harvested at

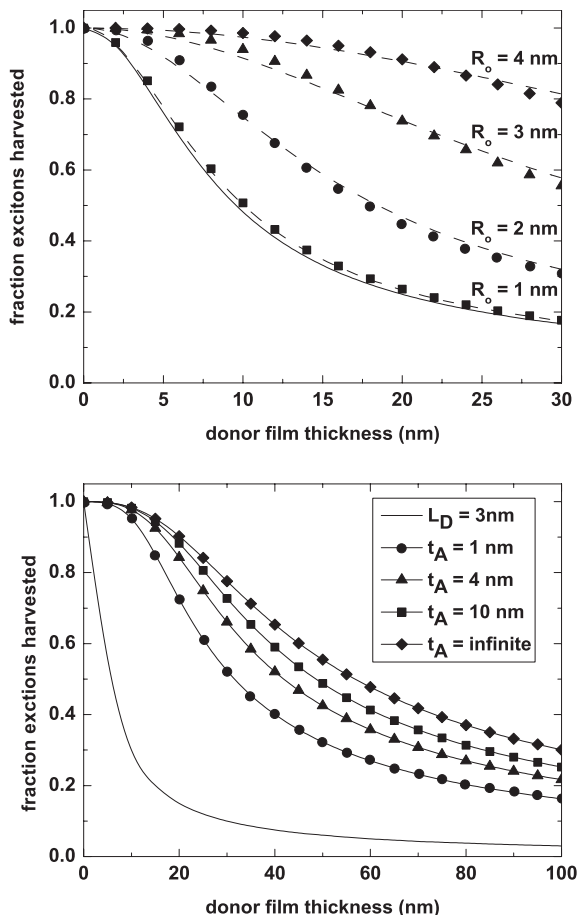


Figure 2. a) Simulations of the fraction of excitons harvested versus energy donor film thickness for diffusion-only with a diffusion length of 5 nm (solid line) as well as diffusion plus hetero-energy transfer with Förster radii of 1 nm (squares), 2 nm (circles), 3 nm (triangles), and 4 nm (diamonds). Dashed lines are simulations incorporating effective diffusion lengths of 5.2 nm, 9.6 nm, 18.8 nm and 35.5 nm. b) Simulations showing the effect of varying the energy acceptor film thickness. Curves are shown for diffusion only with $L_D = 3$ nm (solid black curve), and for acceptor film thicknesses of 1 nm (circles), 4 nm (triangles), 10 nm (squares), and infinite thickness (diamonds) all for $R_0 = 4$ nm.

large distances. As a means of comparison between intrinsic migration and exciton harvesting via long range energy transfer, we can introduce the concept of an “effective diffusion length.”^[16] Each of the exciton harvesting data sets surprisingly can be well-fit with a model incorporating only exciton diffusion whereby an effective diffusion length can be extracted.

When R_0 is 1 nm, energy transfer leads to very little enhancement in exciton harvesting relative to that of intrinsic diffusion with a diffusion length of 5 nm. Consequently, the effective diffusion length for this system is nearly the same as the intrinsic diffusion length. However, if the Förster radius is 2 nm, the effective diffusion length increases to nearly 10 nm, which is close to the value found in the P3HT/PTPTB system previously reported.^[49] At $R_0 = 3$ nm, the effective diffusion length is almost 19 nm and for $R_0 = 4$ nm, the effective diffu-

sion length is almost 36 nm, more than seven times the intrinsic diffusion length. This last case is clearly much larger than just the sum of the intrinsic diffusion length (5 nm) and the Förster radius (4 nm). Adding all pairwise rates between excited donor and possible acceptor chromophores predicts the large enhancement in transfer rate compared to that for one pair of donor and acceptor chromophores.

To experimentally demonstrate efficient long-range energy transfer, we have chosen a highly efficient red emitting polymer, DOW Red, as the energy donor and a highly absorptive low bandgap polymer, a recently reported PTPTB-derivative,^[27] poly(*N*-hexadecan-2-yloxy-carbonyl-2,5-bis(2'-thienyl)-pyrrole-2,1,3-benzothiadiazole), as the energy acceptor. This PTPTB-derivative was designed to have thermally labile solubilizing groups, which made it ideally suited for use in heterostructures since a thin film could be deposited from solution and made insoluble by a simple heat treatment. In this way, well-defined heterostructures with no layer interpenetration could be produced. Figure 1a shows normalized photoluminescence and absorption spectra for the two materials. Using these spectra and assuming a 70% luminescence efficiency for DOW Red and random orientation of the donor and acceptor dipoles, we calculate a Förster radius^[28] of 3.7 nm and an effective diffusion length of 27 nm.

Exciton harvesting as a function of donor film thickness was measured by comparing the DOW Red photoluminescence on glass, where no exciton harvesting occurs, on titania, where excitons are harvested only by intrinsic migration and subsequent electron transfer at the DOW Red/titania interface, and finally on thin films of the energy acceptor PTPTB which can also harvest excitons through long range energy transfer. The fraction of excitons harvested is given simply by:

$$\eta_{\text{exciton}} = \frac{PL_{\text{glass}} - PL_{\text{quench}}}{PL_{\text{glass}}} \quad (3.1)$$

where PL_{glass} and PL_{quench} are the integrated photoluminescence spectra on glass and quenching substrates respectively. Care was taken to avoid overwhelming interference effects as these can dominate the measurement as has been previously shown.^[16,29]

Figure 3 shows exciton harvesting data for DOW Red on titania and for DOW Red on PTPTB. It is clear that more excitons are harvested when PTPTB is incorporated. The continuous curves are models generated from the solutions to Equations 1.1–1.3 assuming a 3 nm (DOW Red on titania) and 27 nm (DOW Red on PTPTB) effective diffusion lengths. These simulations also take into account the optical interference effects that make the generation rate deviate mildly from a constant.^[16] In this system, the intrinsic migration of excitons in DOW Red is extremely limited, as is evidenced by the quenching data on titania, which fits a model incorporating only a 3 nm diffusion length. This is in great contrast to the case where energy transfer can occur. When PTPTB is used as a quencher, more than 50% of the excitons created in a

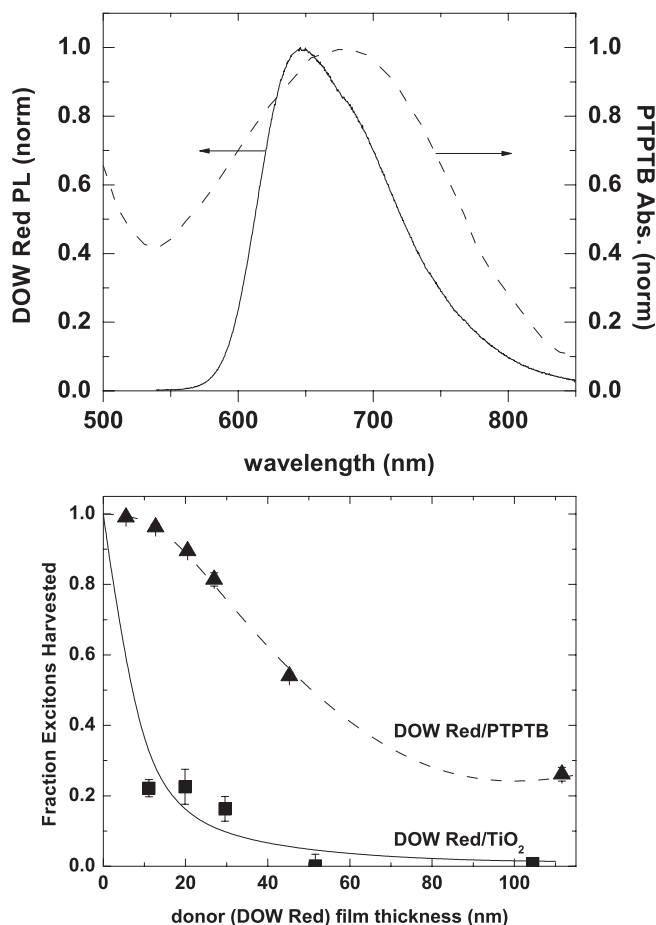


Figure 3. a) Photoluminescence and absorption spectra of energy donor (Dow Red) (solid line) and energy acceptor (PTPTB) (dashed line) showing the strong overlap between the two. b) Fraction of excitons harvested versus DOW Red film thickness on energy acceptor PTPTB (triangles) and on the wide bandgap electron acceptor TiO_2 (squares). The lower solid curve is a simulation corresponding to a diffusion length of 3 nm. The upper dashed curve is a simulation assuming an effective diffusion length of 27 nm which indicates the superior exciton harvesting when long range energy transfer is possible.

50 nm film are harvested to a planar interface and about 90% of the excitons are harvested in a 20 nm film. In this system, when energy transfer can occur and there is strong coulomb coupling, the effective diffusion length is increased by nearly an order of magnitude.

Because all excitons transferred to the energy acceptor must ultimately migrate back to the donor-acceptor interface where they may be split, it is important to investigate the influence of exciton harvesting on energy acceptor film thickness. Figure 2b shows simulations of exciton harvesting for different acceptor film thicknesses.

The solid black curve corresponds to intrinsic diffusion with a diffusion length of 3 nm. Simulations are also shown when energy transfer is included and the energy acceptor film thickness is 1 nm (circles), 4 nm (triangles), 10 nm (squares), and infinite (diamonds) thickness. The largest enhancement is

seen between the simulation of diffusion only and the simulation incorporating energy transfer with a 1 nm thick acceptor layer. Further enhancement is seen, particularly at larger donor film thicknesses, upon increasing the value of the acceptor film thickness to 4 nm and more to 10 nm, which is not far from the predictions of an infinitely thick acceptor film. This demonstrates that the first few monolayers of the energy acceptor film are the most important, and shows that a surface modification scheme whereby the energy acceptor is placed only at an interface to enhance exciton harvesting is potentially a viable approach to engineer better exciton harvesting in ordered bulk heterojunction cells using an inorganic scaffold.

One should be concerned with the amount of energy lost during the exciton harvesting process when incorporating Förster transfer since any loss in energy during the processes between exciton photogeneration and charge carrier extraction in a photovoltaic device directly reduces the maximum achievable photovoltage. Since the absorption spectrum of the acceptor must overlap the emission spectrum of the donor, we argue that incorporating long range energy transfer leads to a lowering of the maximum achievable photovoltage by roughly the difference between absorption and emission energies of the donor material. As exemplified by rigid molecules like the acenes and some ladder polymers, this energy loss can be as low as 0.1 eV.^[50,51]

We have fabricated various planar heterojunction solar cells (DOW Red/PTPTB and MEH-PPV/ TiO_2). In these systems highly efficient exciton harvesting is seen through photoluminescence quenching experiments, but devices show extremely low (<1%) external quantum efficiencies. These quantum efficiencies are even lower than in planar MEH-PPV/ TiO_2 devices where only intrinsic exciton migration can occur and no long range energy transfer is possible. The quantum efficiencies of these devices are low because of the small HOMO offsets between the energy donor and the energy acceptor. Further improvements will surely come by fabricating donor-acceptor heterostructures with well-defined interfaces, proper heterojunction energetics, and through the choice of donor materials with higher photoluminescence efficiencies.

We have shown that long-range resonant energy transfer is a viable scheme to harvest excitons over distances of more than 25 nm. This scheme offers a straightforward route to engineering efficient exciton harvesting by designing strongly coupled donor-acceptor systems and greatly relaxes the domain-size requirements for ordered bulk heterojunction systems. Strong coulomb coupling occurs when the acceptor has a high absorption coefficient, the donor has a high emission efficiency, the transition dipoles are aligned, and the donor emission spectrum overlaps the acceptor absorption spectrum.^[28] Still further improvement should be seen when absorption and emission spectra move to lower energies as the photonic density of states decreases, thereby enhancing non-radiative long range transfer. Experiments on fabricating devices have shown that for efficient exciton splitting, one must ensure there is a sufficient driving force at the heterointerface

following energy transfer. While the long-range energy transfer scheme presented above is intended for use in organic photovoltaics, the ability to harvest excitons nearly 30 nm from an interface should also be of interest for use in OLEDs, organic biosensors, and other novel optoelectronic devices.

Experimental

DOW Red was obtained from the DOW Chemical Company and used as received. MEH-PPV was purchased from ADS, Inc and used as received. Dow Red polymer films of various thicknesses were deposited by spin coating in a nitrogen-filled glove box at 2000 rpm from chlorobenzene solutions. By using solutions with a range of polymer concentrations, we were able to deposit films with thicknesses spanning 5–110 nm. The polymer thickness was measured using a combination of X-ray reflectivity, atomic force microscopy (AFM), and absorption spectroscopy. Polymer films were spin coated onto glass substrates, glass substrates with <5 nm thick titania films (for measuring exciton quenching by intrinsic migration to the titania/polymer interface and subsequent electron transfer), and glass with ~8 nm thick films of thermally treated PTPTB (for measuring exciton quenching by long range energy transfer). Thin titania films were fabricated via a sol-gel route. Titanium(IV)-ethoxide was mixed with a solution of 40:1 ethanol:(concentrated)HCl. Thin films of the titania precursor were spin coated on glass substrates at 2000 rpm and thermally treated at 150 °C in an oven for >8 h to allow condensation and densification of the thin films. Finally these films were calcined at 450 °C to crystallize the titania films. The PTPTB-derivative was synthesized as previously described [27]. Films of the soluble derivative were spin cast from a chloroform solution and subsequent thermal conversion to cleave and evaporate the solubilizing group was performed by heating the films to 250 °C for 30 min in a nitrogen environment. The RMS roughness of all interfaces was found to be less than 1 nm.

532 nm s-polarized light was used for excitation. Photoluminescence spectra were collected using a cooled-CCD camera. We used a sealed chamber to hold the samples in nitrogen to protect the organic films from photodegradation when they were removed from the glove box.

Received: April 11, 2007

Revised: June 13, 2007

Published online: August 31, 2007

- [1] G. Yu, J. Gao, J. C. Hummelen, F. Wudl, A. J. Heeger, *Science* **1995**, *270*, 1789.
- [2] J. J. M. Halls, C. A. Walsh, N. C. Greenham, E. A. Marseglia, R. H. Friend, S. C. Moratti, A. B. Holmes, *Nature* **1995**, *376*, 498.
- [3] C. J. Brabec, G. Zerza, G. Cerullo, S. De Silvestri, S. Luzzati, J. C. Hummelen, S. Sariciftci, *Chem. Phys. Lett.* **2001**, *340*, 232.
- [4] M. M. Wienk, M. G. R. Turbiez, M. P. Struijk, M. Fonrodona, R. A. J. Janssen, *Appl. Phys. Lett.* **2006**, *88*, 153511.
- [5] K. M. Coakley, M. D. McGehee, *Chem. Mater.* **2004**, *16*, 4533.
- [6] K. M. Coakley, Y. X. Liu, M. D. McGehee, K. L. Frindell, G. D. Stucky, *Adv. Funct. Mater.* **2003**, *13*, 301.
- [7] V. Gowrishankar, N. Miller, M. D. McGehee, M. J. Misner, D. Y. Ryu, T. P. Russell, E. Drockenmuller, C. J. Hawker, *Thin Solid Films* **2006**, *513*, 289.
- [8] K. M. Coakley, B. S. Srinivasan, J. M. Ziebarth, C. Goh, Y. X. Liu, M. D. McGehee, *Adv. Funct. Mater.* **2005**, *15*, 1927.
- [9] V. D. Mihailetschi, J. Wildeman, P. W. M. Blom, *Phys. Rev. Lett.* **2005**, *94*, 126602.
- [10] V. D. Mihailetschi, L. J. A. Koster, J. C. Hummelen, P. W. M. Blom, *Phys. Rev. Lett.* **2004**, *93*, 216601.
- [11] P. Peumans, S. R. Forrest, *Chem. Phys. Lett.* **2004**, *398*, 27.
- [12] J. A. Barker, C. M. Ramsdale, N. C. Greenham, *Phys. Rev. B* **2003**, *67*, 75205.
- [13] T. Offermans, S. C. J. Meskers, R. A. J. Janssen, *Chem. Phys.* **2005**, *308*, 125.
- [14] D. C. Olson, J. Piris, R. T. Collins, S. E. Shaheen, D. S. Ginley, *Thin Solid Films* **2006**, *496*, 26.
- [15] C. Goh, K. M. Coakley, M. D. McGehee, *Nano Lett.* **2005**, *5*, 1545.
- [16] S. R. Scully, M. D. McGehee, *J. Appl. Phys.* **2006**, *100*, 034907.
- [17] D. E. Markov, C. Tanase, P. W. M. Blom, J. Wildeman, *Phys. Rev. B* **2005**, *72*, 045217.
- [18] P. Peumans, A. Yakimov, S. Forrest, *J. Appl. Phys.* **2003**, *93*, 3693.
- [19] P. Peumans, S. R. Forrest, *Appl. Phys. Lett.* **2001**, *79*, 126.
- [20] Y. Shao, Y. Yang, *Adv. Mater.* **2005**, *17*, 2841.
- [21] J. W. Arbogast, A. P. Darmanyan, C. S. Foote, Y. Rubin, F. N. Diederich, M. M. Alvarez, S. J. Anz, R. L. Whetten, *J. Phys. Chem.* **1991**, *95*, 11.
- [22] V. Capozzi, G. Casamassima, G. F. Lorusso, A. Minafra, R. Piccolo, T. Trovato, A. Valentini, *Solid State Commun.* **1996**, *98*, 853.
- [23] N. J. Turro, *Modern Molecular Photochemistry*, Benjamin/Cummings, Menlo Park, CA **1978**.
- [24] A. P. Monkman, H. D. Burrows, I. Hamblett, S. Navarathnam, M. Svensson, M. R. Andersson, *J. Chem. Phys.* **2001**, *115*, 9046.
- [25] A. Kohler, D. Beljonne, *Adv. Funct. Mater.* **2004**, *14*, 11.
- [26] Y. X. Liu, M. A. Summers, C. Edder, J. M. J. Fréchet, M. D. McGehee, *Adv. Mater.* **2005**, *17*, 2960.
- [27] C. Edder, P. B. Armstrong, K. B. Prado, J. M. J. Fréchet, *Chem. Commun.* **2006**, 1965.
- [28] T. Forster, *Discuss. Faraday Soc.* **1959**, *27*, 7.
- [29] M. Theander, A. Yartsev, D. Zigmantas, V. Sundström, W. Mammo, M. R. Anderson, O. Inganäs, *Phys. Rev. B* **2000**, *61*, 12957.
- [30] L. C. Chen, L. S. Roman, D. M. Johansson, M. Svensson, M. R. Andersson, R. A. J. Janssen, O. Inganäs, *Adv. Mater.* **2000**, *12*, 1110.
- [31] L. Yu-Xiang, M. A. Summers, S. R. Scully, M. D. McGehee, *J. Appl. Phys.* **2006**, *99*, 93521.
- [32] P. A. van Hal, S. C. J. Meskers, R. A. J. Janssen, *Appl. Phys. A* **2004**, *79*, 41.
- [33] H. Kuhn, *J. Chem. Phys.* **1970**, *53*, 101.
- [34] D. E. Markov, P. W. M. Blom, *Appl. Phys. Lett.* **2005**, *87*, 233511.
- [35] D. E. Markov, P. W. M. Blom, *Phys. Rev. B* **2005**, *72*, 161401.
- [36] J. Hill, S. Y. Heriot, O. Worsfold, T. H. Richardson, A. M. Fox, D. D. C. Bradley, *Phys. Rev. B* **2004**, *69*, 041303.
- [37] T. Del Cano, M. L. Rodriguez-Mendez, R. Aroca, J. A. De Saja, *Mater. Sci. Eng. C* **2002**, *22*, 161.
- [38] K. Ray, H. Nakahara, A. Sakamoto, M. Tasumi, *Chem. Phys. Lett.* **2001**, *342*, 58.
- [39] J. W. Baur, M. F. Rubner, J. R. Reynolds, S. Kim, *Langmuir* **1999**, *15*, 6460.
- [40] P. O. Anikeeva, C. F. Madigan, S. A. Coe-Sullivan, J. S. Steckel, M. G. Bawendi, V. Bulovic, *Chem. Phys. Lett.* **2006**, *424*, 120.
- [41] A. Dhanabalan, J. K. J. van Duren, P. A. van Hal, J. L. J. van Dongen, R. A. J. Janssen, *Adv. Funct. Mater.* **2001**, *11*, 255.
- [42] C. J. Brabec, C. Winder, N. S. Sariciftci, J. C. Hummelen, A. Dhanabalan, P. A. van Hal, R. A. J. Janssen, *Adv. Funct. Mater.* **2002**, *12*, 709.
- [43] N. C. Greenham, I. D. W. Samuel, G. R. Hayes, R. T. Phillips, Y. A. R. R. Kessener, S. C. Moratti, A. B. Holmes, R. H. Friend, *Chem. Phys. Lett.* **1995**, *241*, 89.
- [44] J. E. Kroeze, T. J. Savenije, M. J. W. Vermeulen, J. M. Warman, *J. Phys. Chem. B* **2003**, *107*, 7696.
- [45] M. Scheidler, U. Lemmer, R. Kersting, S. Karg, W. Riess, B. Cleve, R. F. Mahrt, H. Kurz, H. Bassler, E. O. Goebel, P. Thomas, *Phys. Rev. B* **1996**, *54*, 5536.
- [46] C. Im, J. M. Lupton, P. Schouwink, S. Heun, H. Becker, H. Bassler, *J. Chem. Phys.* **2002**, *117*, 1395.
- [47] R. Kersting, U. Lemmer, R. F. Mahrt, K. Leo, H. Kurz, H. Bassler, E. O. Gobel, *Phys. Rev. Lett.* **1993**, *70*, 3820.

- [48] C_A is the acceptor chromophore density which is also used in the calculation of R_0 , since R_0 depends on the molecular absorptivity. Presented a different way we could show that the rate depends only on the total absorption coefficient. As formulated C_A must be consistently used in this equation and in the calculation of R_0 . We choose 8 nm^{-3} .
- [49] Y. X. Liu, M. A. Summers, S. R. Scully, M. D. McGehee, *J. Appl. Phys.* **2006**, *99*, 93 521.
- [50] M. Pope, C. E. Swenberg, *Electronic Processes in Organic Crystals*, Clarendon, Oxford **1982**.
- [51] A. Haugeneder, M. Neges, C. Kallinger, W. Spirkel, U. Lemmer, J. Feldmann, U. Scherf, E. Harth, A. Gugel, K. Mullen, *Phys. Rev. B* **1999**, *59*, 15 346.
-